micromod Partikeltechnologie GmbH

modular designed particles

Publications and Reviews

Technological Applications

Implementation in Life Sciences

magnetic micro- and nanoparticles

www.micromod.de

Product overview

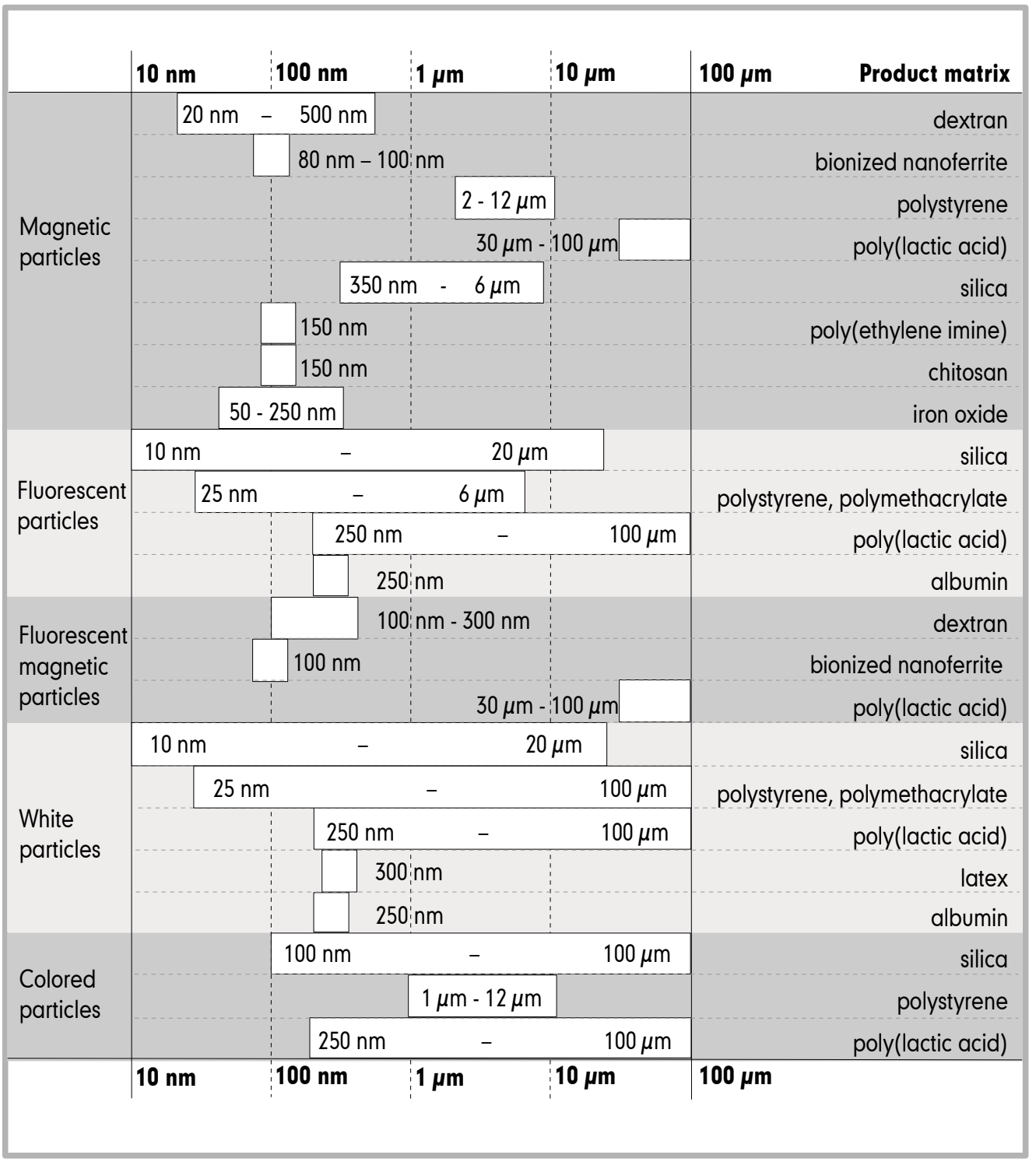

micromod Partikeltechnologie GmbH
Friedrich-Barnewitz-Straße 4, D-18119 Rostock
Tel.:+49 381/54 34 56 10, Fax: +49 381/54 34 56 20
Technical Support Tel.: +49 381/54 34 56 14
E-mail: info@micromod.de, Internet: www.micromod.de

5 Magnetic nanoparticles as contrast agents in Magnetic Resonance Imaging (MRI)

Kerstin Witte[1,2], Cordula Grüttner[2]

[1] *University of Rostock, Institute of Physics, Albert-Einstein-Str. 23, 18059 Rostock, Germany*

[2] *micromod Partikeltechnologie GmbH, Friedrich-Barnewitz-Str. 4, 18119 Rostock, Germany*

5.1 Introduction

The magnetic resonance imaging (MRI) is based on the principle of nuclear magnetic resonance. Certain nuclei possess magnetic moments. In the presence of a magnetic field the magnetic moments undergo precession [1]. The frequency at which the nuclei precess about the magnetic field is known as the Larmor frequency ω_L with:

$$\omega_L = \gamma B_0, \qquad (1)$$

with B_0 being the magnetic field strength and γ being the gyromagnetic ratio. The most important nuclei for magnetic resonance imaging is hydrogen due to the large number in biological tissue [1, 2]. The gyromagnetic ratio for pure hydrogen is $\gamma/2\pi = 42.58$ MHz/T [1].

The net magnetic field a nucleus experiences is a sum not only of the external magnetic fields but also of the field which is generated by electrons surrounding the nucleus. This results in slight shifts of the Larmor frequency of the nucleus and is characteristic for the molecular groups [1]. Therefore by analyzing the different Larmor frequency also different types of tissue can be identified.

A net magnetic field of the oscillating nuclei can be generated by a resonant radio frequency excitation and also be detected by a radio frequency receiver coil [1]. The applied resonant radio frequency excitation is in general a time-varying magnetic field in a plane perpendicular to B_0 leading to a torque of the nuclei [1, 2]. In practice the excitation signal is applied in a pulse a pulse sequence with a duration which is sufficient to obtain a coherent response [2]. However the signal will not persist because of inter-nuclear and inter-molecular forces which will lead to a loss of phase coherence [1]. The precession of the magnetic moment can be described by Bloch equations. The longitudinal relaxation of the magnetization can be described by:

$$M_{II}(t) = M_0 + (M_{II}(0) - M_0)e^{-t/T_1}, \qquad (2)$$

with M_{II} being the longitudinal magnetization, t being the time and T_1 being the longitudinal relaxation time [1]. The longitudinal relaxation time or also spin-lattice relaxation time describes a loss of energy from the system to the surrounding an is related to the dipolar coupling of the nuclei's magnetic moment to its surrounding [2].

The transversal relaxation of the magnetization depends on the phase coherency among the nuclei and can be described by:

$$M_{\perp}(t) = M_{\perp}(0) e^{-t/T_2^{(*)}}, \qquad (3)$$

With $M_{\perp}$ being the transverse magnetization and t being the time [1]. Here two different relaxation times for the transverse relaxation can be distinguished T_2 and T_2^*. As Eq. (3) shows the transverse relaxation describes the loss of coherence among the nuclei and a decay of the signal [1]. In magnetic resonance imaging both offer alternative types of signal contrast among tissues. Spin-echo acquisition provided by T_2 weighting and free induction decay (FID) by T_2^* weighting [1]. The transverse relaxation time T_2 is relatively fast compared to the longitudinal relaxation time and describes the dephasing of the nuclei due to intrinsic factors such as molecular size and tissue type [1]. The dephasing of the nuclei as a result of magnetic field inhomogenities furthermore is described by T_2^* [1, 2]. T_2 and T_2^* are related to one another by:

$$\frac{1}{T_2^*} = \frac{1}{T_2} + \gamma \frac{\Delta B_0}{2}, \qquad (4)$$

with ΔB_0 being the variation of the magnetic field [2].

The images are generated by spatially encoding a nuclear magnetic resonance signal from nuclei present in an object, applying a time varying linear magnetic field gradient. A high resolution and the ability to distinguish soft tissues are the main advantages of the magnetic resonance imaging. In some cases the contrast between different tissues is not sufficient and additional contrast agents are required to achieve sufficient contrast in the magnetic resonance image. Compared to conventional contrast agents, nanoparticle-based contrast agents offer enhanced cellular internalisation and slower clearance from tumors [2]. Furthermore conventional contrast agent can lead to severe adverse effects [3].

The function of the magnetic nanoparticles (MNPs) as agents for contrast enhancement in magnetic resonance imaging can be explained considering the relaxation mechanism in hydrogen nuclei in the presence of the magnetic nanoparticles. The nanoparticles show a strong T_1 relaxation. They also introduce strong inhomogeneities in the local magnetic field due to their high susceptibility, which also reduces the relaxation time T_2^*. Depending on the size of the nanoparticles, a strong influence of the T_1 or T_2 relaxation time can be observed. Smaller magnetic nanoparticles rather tend to shorten the relaxation time T_1, while bigger ones shorten relaxation time T_2, which results in dark areas in magnetic resonance images [4].

Among the broad variety of MNPs in the product assortment of **micromod** the particle types nanomag®-D-spio, nanomag®-CLD-spio, perimag® and BNF provide excellent properties as contrast agent for MRI. Here we provide a short review on third party papers on the application of these particle types for MR imaging in biomedicine and environmental systems. Targeted applications of MNPs for MRI are summarized in chapter 8.

5.2 MR imaging for diagnosis and therapy

5.2.1 Evaluation of the optimal dose of MRI contrast agent

Signal intensity of MR images significantly depends on the concentration of nanoparticles. For clinical studies it is important to find the minimum concentration of iron oxide nanoparticles that produces maximum signal intensity and determines the minimum injection dose. Saharkiz et al. analysed the relationship between the concentration of 20 nm carboxylated nanomag®-D-spio particles and signal intensity using inversion recovery sequence in T1-weighted MR images. The results indicate that the signal intensity is dependent on the concentration of nanoparticles and the inversion time. In addition, the signal intensity increased by increasing the inversion time from 200 to 400 ms for all studied concentrations. The linear relationship between the nanoparticle concentrations and the signal intensity was seen up to 77 µmol Fe/L in 400 ms for long inversion time and 240 µmol Fe/L in 200 ms for short inversion time. The inversion time is an important parameter to consider the relationship between signal intensity and nanoparticle concentrations. An increase in inversion time leads to a decrease in the range of linearity [5]. Furthermore the influence of the coating thickness of nanomag®-D-spio particles with different sizes and polyethylene glycol (PEG) modifications on their relaxivity in MRI was studied. Increments in coating thickness have more influence on relaxivities than differences in the core size of the nanoparticles [6].

5.2.2 Relaxivity measurements for lymphography application

In vitro and *in vivo* investigations in a rat model were performed by Firouznia et al. to investigate the relaxation times T1, T2 and T2* using 20 nm nanomag®-D-spio particles [7]. The relaxation properties of hydrogen nuclei in the presence of the particles at different doses were measured using spin echo and gradient echo imaging protocols. Four different doses of 0.0650 mg/ml, 0.0325 mg/ml, 0.0162 mg/ml and 0.0081 mg/ml particles were used. It was shown that the higher the dose was chosen also all relaxivities increased linearly. Based on these results an optimal protocol was developed for the *in vivo* studies of lymph nodes in rats. Accumulation of particles in the lymph nodes was observed in T_1, T_2 and T_2^* images 4 h after the injection [7].

5.2.3 Cell labelling for MRI tracking

Labelling of cells with MNPs holds promise for monitoring the temporal and spatial migration of stem cells into tissues. It is therefore possible to improve the development of cell tracking strategies for the repair or regeneration of tissues and other cell therapies. Human hematopoietic progenitor cells were labelled with various MRI contrast agents to obtain 1.5 T MR images. Daldrup-Link et al. investigated the amount of different types of magnetic particle based contrast agents and found a maximal internalisation for transferrin conjugated 50 nm nanomag®-CLD-spio particles, followed by ferumoxide, and ferumoxtran. Cell viability and proliferation were not significantly impaired after 7 days of exposure to any MR contrast agent [8].

The feasibility of intranasal administration of neural stem/progenitor cells (NSPCs) was investigated as an alternative, noninvasive, and direct passage for the delivery of stem cells to target malignant gliomas. Tumor-targeting and migratory pathways of murine and human NSPCs were investigated by intravital MRI and in histological time course analyses in different glioblastoma models. Reitz et al. have labelled the NSCPs with nanomag®-D-spio particles for MR imaging. Intranasally administered NSPCs displayed a rapid, targeted tumor tropism with significant numbers of NSPCs accumulating specifically at the intracerebral glioma site within 6 hours after intranasal delivery. This directional distribution of cells accumulating intra- and peritumorally makes the intranasal delivery of NSPCs a promising noninvasive and convenient alternative delivery method for the treatment of malignant gliomas with the possibility of multiple dosing regimens [9].

The influence of protamine sulfate on the labelling efficiency, long-term viability and the iron content stability of mammalian cells that were labelled with 20 nm nanomag®-D-spio particles was studied by *in vitro* MRI measurements over 3 weeks. The labelling efficiency when using protamine sulfate as transfection agent for magnetic cell labelling increased the particle uptake and allowed the cell tracing for a longer duration [10].

Wabler et al. studied the influence of cellular iron content on the MRI contrast of magnetic nanoparticles that were originally developed for hyperthermia treatment of cancer. Human prostate carcinoma DU-145 cells were loaded among other particle types with 100 nm BNF-Starch and 100 nm nanomag®-D-spio at a target concentration of 50 pg Fe/cell using poly-D-lysine transfection reagent. T_2-weighted MRI of serial dilutions of these labelled cells wasperformed at 9.4T and iron content quantification was performed using ICP-MS. For the range of nanoparticle concentrations internalized by cancer cells the signal intensity of T_2-weighted MRI correlates closely with absolute iron concentration associated with the cells. This correlation may benefit applications for cell-based cancer diagnostic by MRI and hyperthermia therapy [11].

Cell penetrating peptides (CPPs) have been widely used to increase the cellular uptake of nanoparticles. Cavalli et al. have functionalized nanomag®-CLD-spio particles with surface benzaldehyde groups for conjugation of a g-amino-proline-derived peptide. This new peptide-particle conjugate was found to have a remarkably higher cell penetrating capability in comparison to established TAT-peptide functionalized MNPs. The high level of uptake into HeLa cells was demonstrated by MRI studies to provide a decrease in the T2 of labelled cells [12].

5.2.4 Noninvasive MRI of an asthma biomarker in the lung using PEG-functionalized MNPs

Asthma is a complex and chronic pulmonary disease characterized by airway hyper-responsiveness and inflammation, as well as underlying structural changes to the airways. Al Faraj et al. present a promising therapeutic approach to give the additional relief required for asthma patients. IL4 and IL13 were simultaneously inhibited via the common receptor chain IL4Rα to block adequately their biologic effects.

Nanomag®-CLD-spio were conjugated with anti-IL4Rα blocking antibodies via polyethylene glycol (PEG) polymers of different lengths. The delivery of these blocking antibodies to the inflammatory sites in the lung via the developed nanocarriers was assessed using noninvasive free-breathing pulmonary MRI. The anti-IL4Rα-conjugated nanocarriers have been confirmed to be efficient in targeting key inflammatory cells during chronic lung inflammation following intrapulmonary administration in the lung of ovalbumin-challenged asthmatic mice [13]. In another approach the targeting of MNPs to the lung after intravenous administration of BNF-Starch particles should be increased. To achieve a higher pulmonary delivery, high-energy flexible magnets were optimized and externally applied to a specific region of mouse lung. A free-breathing MRI protocol was then optimized to allow noninvasive monitoring [14].

5.2.5 MRI detection of protease producing tumor derived cells by proteolytic actuation of nanoparticle self-assembly

Inspired by the idea of initiating assembly by enzymatic removal of inhibitors, Harris et al. demonstrated with peptide–polymer chemistry that inorganic nanoparticles may be functionalized to exist in a "latent" state until triggered by a protease to self-assemble. The binding of biotin and neutravidin coated 50 nm nanomag®-D-spio particles was inhibited with polyethylene glycol (PEG) polymers that may be proteolytically removed to initiate assembly by matrix metalloproteinase-2 (MMP-2), a protease correlated with cancer invasion, angiogenesis and metastasis. MMP-2 initiated assembly amplifies the transverse (T2) relaxation of nanoparticle suspensions in MRI, enables magnetic manipulation with external fields, and allows MRI detection of tumor-derived cells that produce the protease. This general approach may enable site-selective immobilization and enhanced image contrast in regions of tumor invasion *in vivo [15]*.

5.3 MR imaging of MNPs in environmental systems

In biofilm research, the investigation of the biofilms' physical structure is of high relevance for the understanding of mass transport processes. However, commonly used imaging techniques for biofilm imaging such as confocal laser scanning microscopy or electron microscopy rarely visualize the *real* biofilm due to their invasiveness and destructiveness. MRI represents the ideal tool to image the biofilm *in situ*, *non-invasively* and *non-destructively* with a spatial resolution of several 10 µm. To gain specific structural and functional information, a variety of MRI contrast agents was applied with different properties for the first time. Beside molecular contrast agentsdifferent types of MNPs were studied. Thereby the particle type (nanomag®-D-spio and BNF), the size (20 nm and 80 nm), the matrix material (dextran or starch) and the surface functionalities of the MNPs (plain, COOH, NH2) were varied. Results elucidate the interactions between the biofilms' surface and the contrast agents and open a new field for biotechnological applications by functional contrast enhancement [16].

The widespread application of MNPs in biomedicine might result in their release into the environment, where their fate will notably depend on their stability and on their transport behaviour in soil and aquatic systems. The successful application of MNPs for groundwater remediation also significantly depends on their mobility after the injection. Cuny et al. investigated the mobility of various MNPs in water-saturated porous media. Laboratory-scale transport experiments were conducted using columns packed with quartz sand as model solid phase. The same set of nanomag®-D-spio and BNF particles as in [16] was selected to study the influence of primary particle size and surface functionalization on particle mobility. MRI provided detailed spatially resolved information complementary to the quantitative detection of the particle breakthrough curves. The approach can be transferred to other porous systems and contributes to a better understanding of particle transport in environmental porous media and porous media in technical applications [17].

References

[1] Prasad, P.V., *Magnetic resonance imaging: methods and biologic applications*. 2006: Springer Science & Business Media.

[2] Pankhurst, Q.A., et al., *Applications of magnetic nanoparticles in biomedicine.* Journal of physics D: Applied physics, 2003. **36**(13): p. R167.

[3] Colombo, M., et al., *Biological applications of magnetic nanoparticles.* Chem Soc Rev, 2012. **41**(11): p. 4306-34.

[4] Geraldes, C.F. and S. Laurent, *Classification and basic properties of contrast agents for magnetic resonance imaging.* Contrast media & molecular imaging, 2009. **4**(1): p. 1-23.

[5] Saharkhiz, H., et al., *The effect of inversion time on the relationship between iron oxide nanoparticles concentration and signal intensity in T1-weighted MR images.* Iranian Journal of Radiology, 2014. **11**(2).

[6] Hajesmaeelzadeh, F., et al., *Effect of coating thickness of iron oxide nanoparticles on their relaxivity in the MRI.* Iranian Journal of Basic Medical Sciences, 2016. **19**(2): p. 166-171.

[7] Firouznia, K., et al., *MR relaxivity measurement of iron oxide nano-particles for MR lymphography applications.* Pakistan Journal of Biological Sciences: PJBS, 2008. **11**(4): p. 607-612.

[8] Daldrup-Link, H.E., et al., *Targeting of Hematopoietic Progenitor Cells with MR Contrast Agents 1.* Radiology, 2003. **228**(3): p. 760-767.

[9] Reitz, M., et al., *Intranasal delivery of neural stem/progenitor cells: a noninvasive passage to target intracerebral glioma.* Stem cells translational medicine, 2012. **1**(12): p. 866-873.

[10] Shanehsazzadeh, S., et al., *Evaluating the effect of ultrasmall superparamagnetic iron oxide nanoparticles for a long-term magnetic cell labeling.* Journal of Medical Physics, 2013. **38**(1): p. 34-40.

[11] Wabler, M., et al., *Magnetic resonance imaging contrast of iron oxide nanoparticles developed for hyperthermia is dominated by iron content.* International Journal of Hyperthermia, 2014. **30**(3): p. 192-200.

[12] Cavalli, S., et al., *Efficient gamma-amino-proline-derived cell penetrating peptide-superparamagnetic iron oxide nanoparticle conjugates via aniline-catalyzed oxime chemistry as bimodal imaging nanoagents.* Chemical Communications, 2012. **48**(43): p. 5322-5324.

[13] Al Faraj, A., et al., *Specific targeting and noninvasive magnetic resonance imaging of an asthma biomarker in the lung using polyethylene glycol functionalized magnetic nanocarriers.* Contrast media & molecular imaging, 2015.

[14] Al Faraj, A., et al., *Enhanced magnetic delivery of superparamagnetic iron oxide nanoparticles to the lung monitored using noninvasive MR.* Journal of Nanoparticle Research, 2014. **16**(10): p. 1-11.

[15] Harris, T.J., et al., *Proteolytic Actuation of Nanoparticle Self-Assembly.* Angewandte Chemie, 2006. **118**(19): p. 3233-3237.

[16] Ranzinger, F., et al., *Direct surface visualization of biofilms with high spin coordination clusters using Magnetic Resonance Imaging.* Acta biomaterialia, 2016. **31**: p. 167-177.

[17] Cuny, L., et al., *Magnetic resonance imaging reveals detailed spatial and temporal distribution of iron-based nanoparticles transported through water-saturated porous media.* Journal of contaminant hydrology, 2015. **182**: p. 51-62.

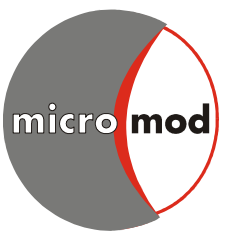

Editor:
micromod Partikeltechnologie GmbH

Registergericht: Amtsgericht Rostock HRB 5837
Steuernummer: 4079/114/03352
Ust-Id Nr. (Vat No.): DE167349493

Compilation date - May the 10th, 2017
micromod Partikeltechnologie GmbH

www.micromod.de